RSC Advances

PAPER

View Article Online
View Journal | View Issue

Cite this: *RSC Adv.*, 2023, **13**, 2984

Preparation of graphitized carbon by the corn straw liquefaction method

Shuo Dai,[a] Yao Fu,[a] Peng He,[a] Li Mu,*[a] Pengfei Liu[b] and Yuyan Zhang[c]

Received 18th November 2022
Accepted 3rd January 2023

DOI: 10.1039/d2ra07352h

rsc.li/rsc-advances

Corn straw-based graphitized carbon was prepared by carbonization and a catalyzed graphitization method using corn straw as the raw material and catalytic liquefaction technology. A mixture of polyethylene glycol (PEG200) compounded with glycerol in the mass ratio of 7 : 3 was used as the liquefied agent, meanwhile 0.3 g of hydroxydiethylidene glycolic acid acted as the liquefied catalyst. The liquefied products were treated *via* carbonization and graphitization processes to form graphitized carbon. The graphitized carbon showed better graphitization, a microscopic lamellar structure, and smaller defects, when the carbonized temperature was 600 °C, graphitization temperature 850 °C, and the catalyst was ferric acetylacetonate at a concentration of 7.0 mmol g^{-1}. The corn straw-based graphitized carbon yield reached 22.20%.

1 Introduction

As a renewable biomass resource, corn straw is widely distributed in nature and has abundant resources. The main components of corn straw are cellulose, hemicellulose, and lignin,[1,2] and is a kind of energy material that human beings have been using since long ago; however, how to deal with straw crops reasonably has become one of the hot spots to be solved among current environmental pollution problems. The preparation of graphite materials from corn straw can realize the high value utilization of corn straw to a certain extent.

At present, the main technologies for the liquefaction method of corn straw are microwave chemical liquefaction,[3,4] catalyzed liquefaction,[5,6] hydrothermal liquefaction,[7–10] rapid pyrolytic liquefaction,[11] liquefaction by enzymatic fermentation,[12–14] and super/near-critical technology.[15–17] There are many studies using various liquefaction technologies to process corn straw to obtain direct products, such as bio-oil, ethanol, resins, and polyurethane, but the liquefaction technology seems to be face certain barriers. On the one hand, some liquefied reactions require the catalysts to promote the reaction progress and get more favorable factors to prepare the corresponding products by increasing the liquefaction rate. In this case, strong acids and bases, such as concentrated sulfuric acid, are used as catalysts, which inevitably requires consideration of the impact of the use of strong corrosive reagents in experimental operations, waste liquid disposal, and the environment. On the other hand, when a relatively mild catalyst is added to the reaction system, the liquefaction effect is reduced or even greatly diminished compared to the former. Therefore, how to balance these two differentiated situations through improvement of the experimental conditions and technical means to be able to use more moderate conditions and reagents to prepare higher quality, high-performance products will inevitably be a subject for future long-term investigation and exploration.

In the experiment, polyethylene glycol (PEG200) compounded with glycerol in the mass ratio of 7 : 3 was used as the liquefied agent for experimental investigation of the liquefaction process of corn straw. After corn straw is liquefied, the liquefied products are used as raw materials for graphitization for two main reasons. One is that corn straw contains hemicellulose and lignin, which are unfavorable for the formation of thin graphene materials.[18] Being liquefied, the three major components of corn straw are degraded to varying degrees, which is beneficial for the recombination of graphitized carbon. Second, the normal biomass will be degassed and dehydrated during the carbonization process, while the remaining parts that are difficult to be liquefied during the liquefaction process will be shaped into a stronger carbon skeleton after carbonization, and the graphitization effect will be better. In this study, graphitic carbon materials were prepared from inexpensive woody biomass feedstock corn straw using combinatorial technological innovation to provide the base material for the exfoliation of high-quality graphene.

2 Materials and instruments

2.1 Experimental materials and reagents

Corn straw powder was provided by Jilin COFCO Biochemical Energy Sales Co. Ltd, China. Polyethylene glycol 200 (PEG 200)

[a]*College of Food Science and Engineering, Changchun University, Changchun, Jilin, 130022, China. E-mail: mul@ccu.edu.cn*

[b]*School of Chemical Engineering in Changchun University of Technology, Changchun, Jilin, 130023, China*

[c]*North China Electric Power University, Beijing, 071003, China*

was obtained from Tianjin Guangfu Fine Chemical Research Institute. Glycerol (GL) and anhydrous ethanol were ordered from Shandong Jinan Mingliang Chemical Co. Ltd. Hydroxyethylene bisphosphate (HEDP), ferric acetylacetonate, ferrocene, ferric oxalate, and ferric citrate were ordered from Shanghai Macklin Biochemical Co., Ltd.

2.2 Experimental instruments

An electronic analytical balance (Huazhi Electronic Technology Co., Ltd, China) was used to weigh the materials and samples. A vacuum drying oven (Shanghai Xinmiao Medical Equipment Co., Ltd, China) was used to remove water from the materials. A tube furnace (Luoyang Pure Green Furnace Co., Ltd, China) was used to heat the materials and samples.

Powder XRD patterns were obtained using a BRUKER diffractometer with Cu radiation ($\lambda = 0.15418$ nm). Scanning electron microscopy (SEM) was done on a JSM-7610F electron microscope. Raman spectroscopy was performed on a LabRAM HR Evolution system. Fourier transform infrared spectroscopy (FTIR) was done on a NICOLET IS 10 system.

Brunauer–Emmer–Teller (BET) analysis was performed with a Quantachrome® ASiQwin™, Quantachrome Instruments v2.02 with nitrogen (N_2) gas used as an absorptive for the determination of the surface area.

3 Experimental methods and mechanisms

3.1 Principle of the liquefaction of the polyhydroxy alcohols

The direct liquefaction process of corn straw is a complex reaction process, consisting of the alcoholysis reaction with cellulose, hemicellulose, and lignin used as the reaction substances, the phenolic condensation reaction of liquefaction products, the hydroxylaldehyde condensation reaction, and the esterification condensation reaction. However, under relatively mild reaction conditions, the liquefaction reaction has some priority over the condensation reaction of the liquefaction products.[19]

3.2 Corn straw liquefaction process

The liquefaction process of corn straw was the first step in our experiments, and its liquefied products were the raw materials for the subsequent carbonization and graphitization processes. This study focused on investigating the feasibility of preparing graphitic carbon materials from corn straw after liquefaction and the degree of graphitization of the products. Since the solid–liquid ratio factor in the liquefaction process has a large influence on the state of the graphitized products, the liquefaction experimental conditions were referred to the relevant literature,[20] and only the solid–liquid ratio was initially investigated for its influence on the liquefied yield. The solid–liquid ratio was then analyzed as a subsequent factor affecting the degree of graphitization.

First, 10.0 g of corn straw powder was weighed and placed into a high-pressure reactor, with liquefied agent added that was compounded by polyethylene glycol (PEG200) and glycerol in a mass ratio of 7 : 3, with 0.3 g of hydroxyethylene bisphosphate also added as the catalyst in to the high-pressure reactor. Then, the high-pressure reactor was tightened and put into a preheated vacuum drying oven for the liquefaction reaction, with a reaction temperature of 140 °C and reaction time of 5 h. Then, the high-pressure reactor was cooled to room temperature after finishing the experimental reaction.

Eqn (1) was used to calculate the liquefaction yield of corn straw.

$$Y_{\text{liquefaction yield}} = \frac{M_{\text{total liquefied mass}} - M_{\text{liquefaction residues mass}}}{M_{\text{total liquefied mass}}} \times 100\% \quad (1)$$

3.3 Principle of preparing graphitized carbon from the liquefaction products

Corn straw liquefied products as raw material underwent carbonization and graphitization with an iron-based catalyst and suitable reaction temperature and the system was blown by N_2 gas. The iron-based catalysts decompose into the liquid phase, and through the carburization of the iron-based catalyst flow from the interstices to encapsulate the carbon element in corn straw to form layers between the carbon and polymers with multiple groups.[21,22] The dissolved carbon gradually forms fixed graphitized carbon during the annealing process to room temperature, and at the same time, the iron elements agglomerate on and around the graphite carbon surface due to cooling to appear as irregular agglomerates. Then, the graphitized product was washed with hydrochloric acid solution to remove the iron elements, until finally the corn straw-based graphitized carbon is obtained (Fig. 1).

3.4 Carbonization of the liquefied products

The liquefied products of corn straw were weighed and placed in a corundum crucible, then the crucible was put into the middle section of the tube furnace, in which the liquefied products were changed, under the reaction temperatures of 400 °C, 500 °C, 600 °C, at a temperature increase rate of 5 °C min^{-1}, while the process of reaction was aiding by blowing N_2 gas in to the tube furnace. When reaction was terminated, the temperature was kept at a constant set temperature for 1.0 h. The obtained calcination product was soaked in 20 wt% anhydrous ethanol, ground, and then filtered by extraction. The carbonized liquefied products were obtained after drying at 80 °C for 12.0 h.

Eqn (2) was used to calculate the carbonization yield.

$$Y_{\text{carbonization yield}} = \frac{m_{\text{carbonizated products mass}}}{m_{\text{liquefied products mass}}} \times 100\% \quad (2)$$

3.5 Graphitization of the carbonized products

First, 1.0 g of carbonized products was weighed, and mixed respectively with 7.0 mmol of the iron-based catalyst, which was one of the four different iron-based catalysts, namely ferric

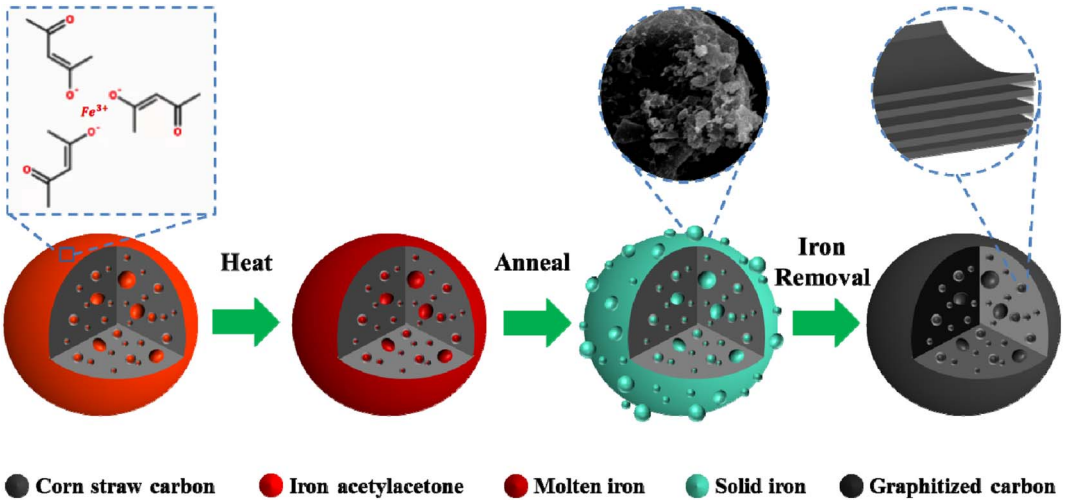

Fig. 1 Principle simulation diagram of the catalytic graphitization process.

acetylacetonate, ferrocene, ferric oxalate, and ferric citrate. According to the carbonization method in Section 3.4, when the reaction temperature was 850 °C, it was held there for one hour, and then the calcination products were removed by grinding, soaking in hydrochloric acid solution, followed by ultrasonication for 1 h to remove the iron element. Graphitized carbon was obtained after drying at 80 °C for 12.0 h, and calculated according to the following equation.

$$Y_{\text{graphitized carbon yield}} = \frac{M_{\text{graphitized carbon mass}}}{M_{\text{corn straw initial mass}}} \times 100\% \quad (3)$$

4 Results and discussion

4.1 Effect of the solid–liquid ratio on the liquefied corn straw

According to the liquefaction method of corn straw outlined in Section 3.2, with the increase in the solid–liquid ratio, the liquefaction yield of corn straw showed an increasing trend. When the solid–liquid ratio increased from 1 : 2 to 1 : 3, the liquefaction yield of corn straw reached a maximum of 24.71% as shown in Fig. 2.

4.2 Effect of the solid–liquid ratio on the carbonization of the liquefied products

After the liquefied products of corn straw were treated in line with the processes described in Sections 3.2 and 3.4, with the increase in the solid–liquid ratio, the carbonization yield overall decreased, as seen in Fig. 3, because when the solid–liquid ratio increased, there would be more of the liquid part of the mixed liquefaction products and less of the solid carbon products after the liquefied products of corn straw were heated and charred, so the carbonization yield would drop.

4.3 Single-factor experiment on graphitization

4.3.1 Effect of the solid–liquid ratio. According to the treatment process of corn straw outlined in Sections 3.2, 3.4 and 3.5, the graphitization temperature was maintained at 850 °C

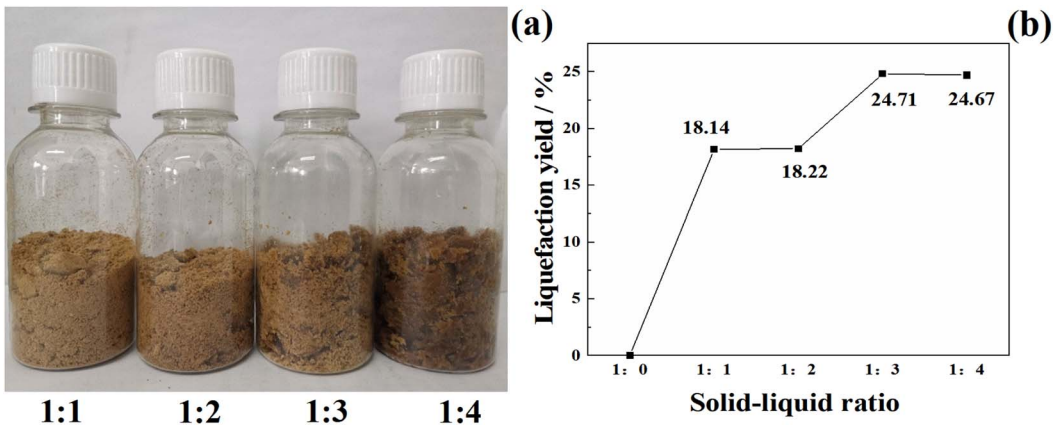

Fig. 2 Photograph of the mixed liquefaction products of corn straw with solid–liquid ratios of 1 : 1–1 : 4 (a). Effect of the solid–liquid ratio on the liquefaction yield of corn straw (b).

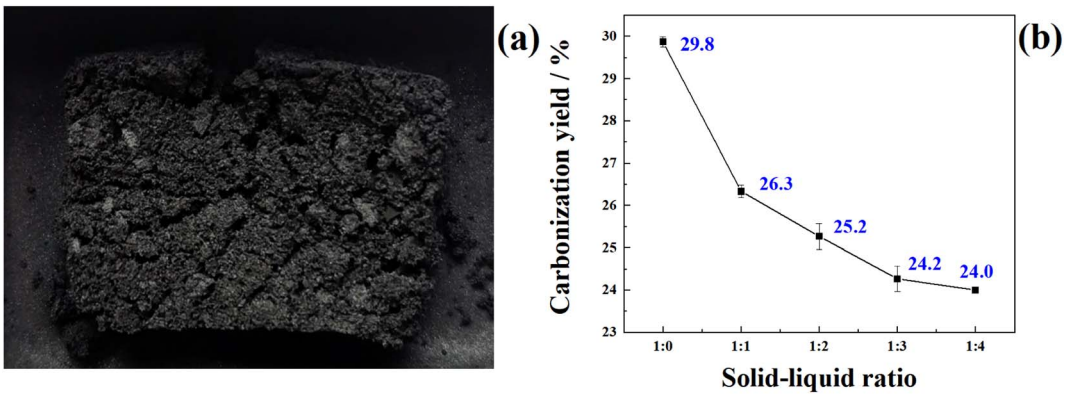

Fig. 3 Photograph of the completely carbonized product with a solid–liquid ratio 1 : 2 (a). Effect of the solid–liquid ratio on the carbonization yield (b).

and the solid–liquid ratio of the liquefied products was changed in the ratios 1 : 0, 1 : 1, 1 : 2, 1 : 3, 1 : 4, and the residues were detected by X-ray diffraction and Raman spectroscopy. The resulting chromatograms are shown in Fig. 4.

It was found that degree of graphitization of the residues were different for the different solid–liquid ratios. The first peak around 1000 to 1400 cm^{-1} was the D peak, and the peak around 1400 to 1600 cm^{-1} was the G peak. The I_D/I_G value was used to indicate the degree of graphitization,[23] whereby the smaller the ratio of I_D/I_G, the better the graphitization degree. When the solid–liquid ratio was 1 : 2, I_D/I_G was 0.7314, which was the smallest, with the graphitized degree obvious from Fig. 4(a).

The characteristic peaks of the X-ray diffraction of the residues appearing around 25°–28°, corresponding to the (002) crystal plane of the sample. When the solid–liquid ratio was 1 : 2, the spectrum of the residues (Fig. 4(b)) had the sharpest (002) crystalline peak with a 2θ of 26.38°, which showed the best graphitization degree. The above data reflected by X-ray diffraction corresponded to the Raman spectra. Therefore, the most suitable solid–liquid ratio of the liquefied products for graphitization could be determined as 1 : 2.

4.3.2 Effect of the catalyst concentration. The graphitization process of the corn straw carbonized products was conducted under different catalyst concentrations of 1.0, 4.0, 7.0, and 9.0 mmol g^{-1}, and the resulting chromatograms are shown in Fig. 5, according to the treatment process of corn straw in Sections 3.2, 3.4 and 3.5.

It was shown that with the increase in the catalyst concentration, the I_D/I_G values tended to decrease and then increase, as shown in Fig. 5(a). When the catalyst was 7.0 mmol g^{-1}, I_D/I_G was 0.7314, which was the smallest and the graphitized degree was the best. When the catalyst concentration was 9.0 mmol g^{-1}, the D and G peaks were higher, but the I_D/I_G values were larger and greater than 1. This means the graphitized degree was poor and defective, which might be due to the catalyst concentration reaching the supersaturated state and having a negative effect during characterization.

As shown in Fig. 5(b), when the catalyst concentration was 1.0 mmol g^{-1}, the catalytic effect was not obvious. With the increase in the catalyst concentration, the graphitized carbon showed X-ray diffraction peaks around 25°–28°. When the catalyst concentration was 7.0 mmol g^{-1}, the (002) crystalline peak of the residuals was the sharpest, so the optimal catalyst concentration for graphitization could be determined as 7.0 mmol g^{-1}.

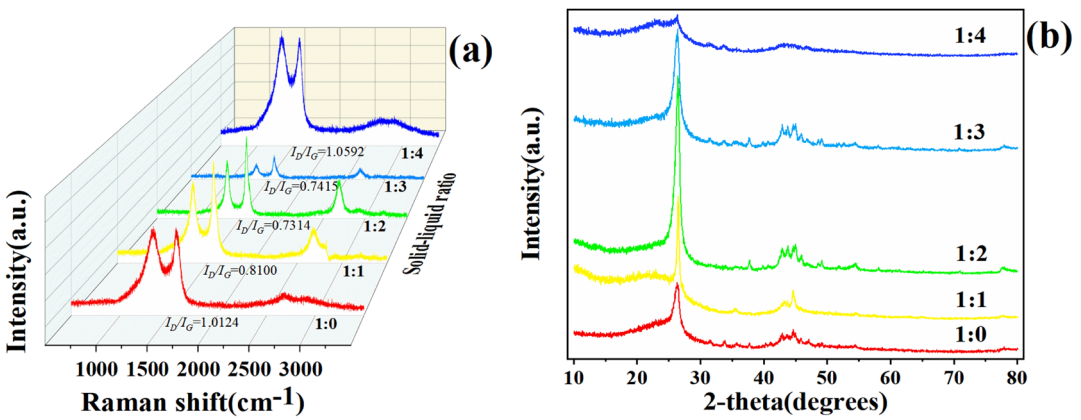

Fig. 4 Raman spectra of the residues in different solid–liquid ratios (a). X-ray diffraction patterns of the residues in different solid–liquid ratios (b).

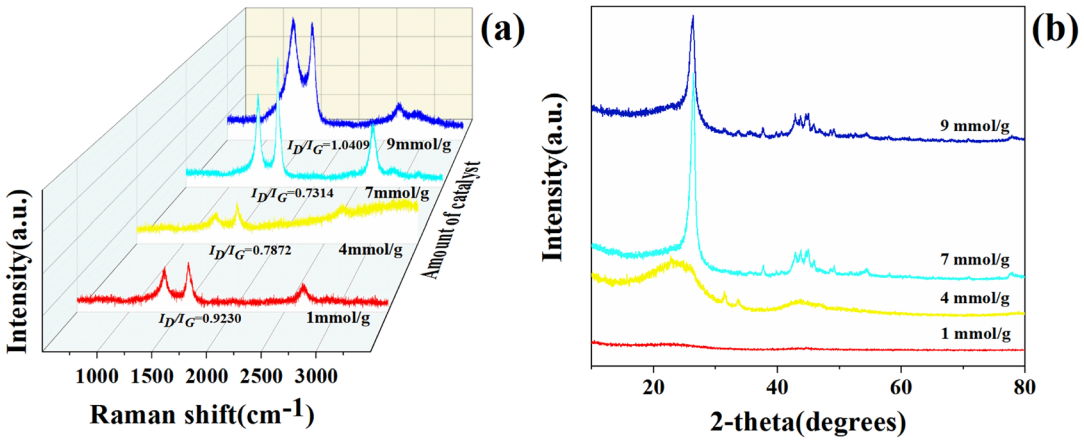

Fig. 5 Raman spectra of the residues in different catalyst concentrations (a). X-ray diffraction patterns of the residues in different catalyst concentrations (b).

4.3.3 Effect of the graphitization temperature. During the graphitized process in Section 3.4, graphitized temperatures of 750 °C, 800 °C, 850 °C, and 900 °C were used. The resulting chromatograms of the residues are shown in Fig. 6. When the graphitization temperature was in the range of 750–900 °C, the I_D/I_G value decreased first and then increased, which showed that controlling the graphitization temperature had some effect on the graphitization process. When the temperature continued to rise to 900 °C, the I_D/I_G value was larger and greater than 1, as shown in Fig. 6(a), and the graphitized degree became worse. Therefore, the graphitization temperature of 850 °C was selected as the optimal temperature for the experiments. This conclusion was consistent with the XRD patterns in Fig. 6(b).

4.3.4 Effect of the catalyst. The iron catalyst selected in the experiment was mainly obtained through a similar alloying process between the metal particles and corn straw carbon in the reaction, which could effectively reduce the melting point. Under the action of temperature and nitrogen, the iron-based catalyst decomposes into a liquid phase, then flows in from the gap through the carburization of iron, and enwraps the corn straw carbon particles, forming layers between the carbon and the polymers of various groups.[24]

The graphitization catalysts were changed to ferric acetylacetonate, ferrocene, ferric oxalate and ferric citrate under the conditions of 1.0 g of the carbon of the corn straw liquefaction product, 1 : 2 solid–liquid ratio of corn straw liquefaction products, 7.0 mmol g^{-1} catalyst, and 1.0 h of holding time at 850 °C for graphitization. Analytical graphs of the Raman spectra and X-ray diffraction were obtained under the corresponding catalysts, respectively.

The I_D/I_G values of graphitized carbon catalyzed by the ferric oxalate, ferrocene, and ferric citrate catalysts were larger and all greater than the value of 1, indicating that its graphitized degree was poor and the graphitized carbon defects were large. In the system with ferric acetylacetonate as a catalyst, the I_D/I_G value was 0.7314 in Fig. 7(a). From Fig. 7(b), graphitized carbon characteristic peaks on the X-ray diffraction patterns are not shown, while the catalyst was one of the three catalysts, *i.e.* ferric oxalate, ferrocene, and ferric citrate, corresponding to the data reflected by the Raman spectra. Therefore ferric acetylacetonate as the graphitization catalyst had a better effect than the others.

The isotherms and pore-size distribution curves for the adsorption and desorption of the corn straw-based graphitized

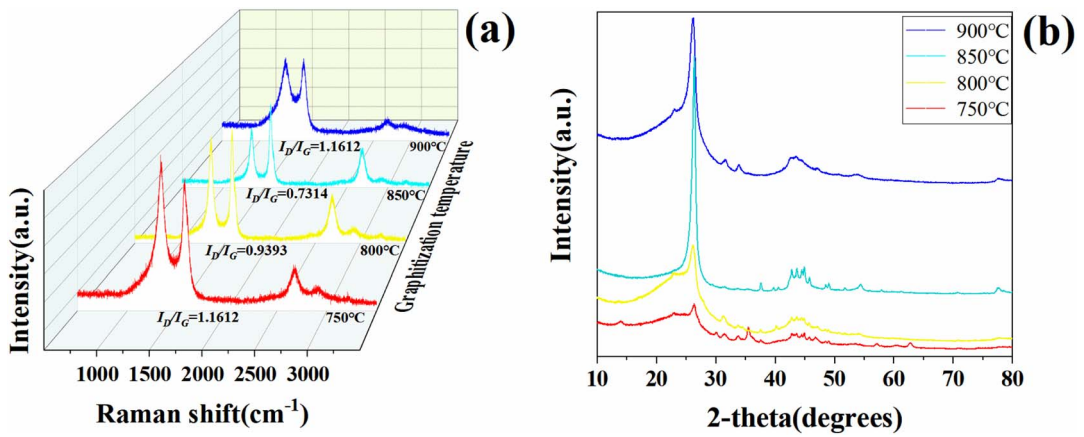

Fig. 6 Raman spectra for the different graphitization temperatures (a). X-ray diffraction patterns for the different graphitization temperatures (b).

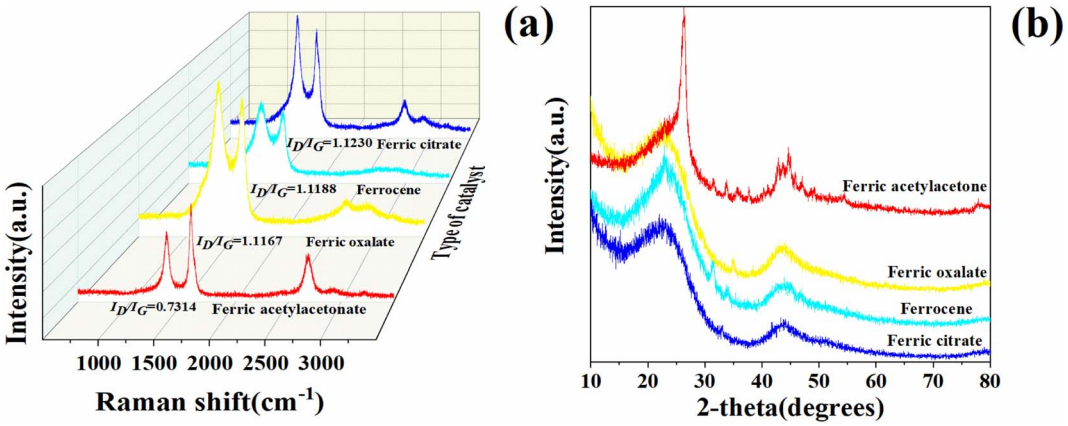

Fig. 7 Raman spectra of graphitized carbon obtained with different catalysts (a). X-ray diffraction patterns of graphitized carbon obtained with different graphitization catalysts (b).

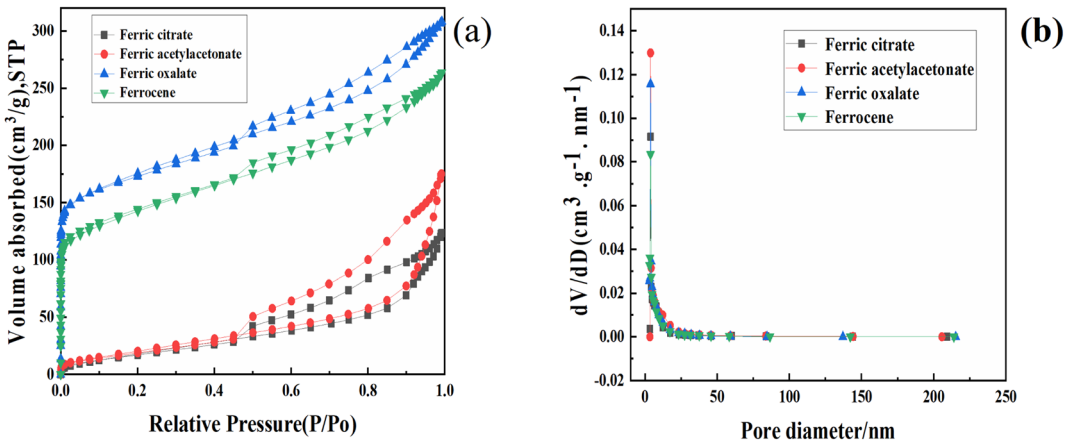

Fig. 8 N_2 adsorption/desorption isotherms (a). Corresponding pore-size distribution (b).

carbon obtained from the four iron-based catalysts are shown in Fig. 8. The curves coincided with type IV adsorption isotherm curves, with capillary coalescence present in the high-pressure region, while the adsorption–desorption curves did not overlap, indicating the presence of some mesopores. The H3-type hysteresis loop was also evident in the diagram, indicating that the materials obtained were in the form of loose flakes or granules, which was consistent with the SEM analysis. This indicated that the biochar produced was a mesoporous material. As can also be seen in Fig. 8(b), the pores of the material were mostly below 3.9 nm.

4.3.5 Effect of the solid–liquid ratio on graphitized products. It was shown that with the increase in the solid–liquid ratio, the graphitization carbon yield decreased overall, as shown in Fig. 9, after the carbonized products of corn straw were treated as outlined in Section 3.5. When the solid–liquid ratios were 1 : 0 and 1 : 1, the graphitized carbon yields were 22.89% and 22.60%, respectively. Although the two values were more than 22.20%, which corresponded to a solid–liquid ratio of 1 : 2, it could be found that the graphitization degree was not obvious by analysis of a higher I_D/I_G value.

4.4 Structural characterization of the residues

4.4.1 SEM. Scanning electron microscopy (SEM) images of the residues are shown in Fig. 10. The SEM images of the corn straw showed it was in the shape of fibrous rods (Fig. 9(a)). The microscopic characteristic structure of the corn straw was changed after the liquefaction and graphitization process, as shown in Fig. 10(b and c). From Fig. 10(d), a microscopic appearance of the graphitized carbon wrapped in agglomerates after the action of ferric acetylacetonate catalyst could be seen. After soaking in hydrochloric acid solution (Fig. 10(e and f)), the graphitization residues were graphitized carbon with lamellar characteristics.

4.4.2 XRD. Corn straw is mainly composed of cellulose, hemicellulose, and lignin. Cellulose is a microfibrillar, which is composed of long bundles of cellulose molecules arranged in parallel between bundles, and is formed by connecting crystalline regions and amorphous regions. If cellulose molecules have a certain regular arrangement, they will form crystalline regions, showing strong diffraction peaks in the XRD diagram. The amorphous region is located between the crystalline regions and has no obvious boundary with the crystalline

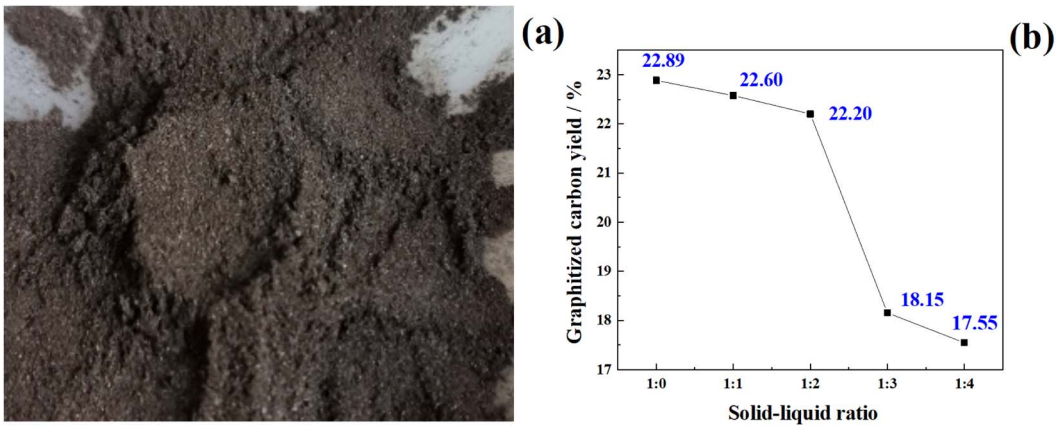

Fig. 9 Photograph of the graphitized carbon (a). Effect of the solid–liquid ratio on the graphitized carbon yield (b).

region. The crystalline region of cellulose is often interrupted by hemicellulose and is jointly embedded in lignin. Here, it could be seen from Fig. 10 (corn straw) that strong diffraction peaks appeared at 21.85°, and weak diffraction peaks appeared at 15.05°.[25] As seen in the spectra of the graphitized carbon in Fig. 11, the graphitized characteristic peak near 25°–30° corresponded to the (002) crystal plane of the sample, and the characteristic peak was sharp with a 2θ of 26.38°, so the graphitized degree was obvious. It was also shown by the X-ray diffraction pattern that the corn straw crystalline shape *via* liquefaction and graphitization processes was changed, which was also consistent with the results obtained from the SEM images analysis.

4.4.3 FT-IR. Spectrograms of the residues of the corn straw-based graphitized carbon and corn straw are shown in Fig. 12. The corn straw was treated to change the graphitized carbon products, for which the FTIR spectra showed many smooth, absorption peaks, whose intensity was apparently presented as weak. The β-1,4-glycosidic bonds of corn straw were broken, and the main components (cellulose, hemicellulose, lignin) were changed and a new carbon skeleton was reconstituted. The absorption peaks in the range of 1000–1250 cm^{-1} were infrared symmetric characteristic peaks of the ether bonds. The absorption peak of the residues after graphitization in this range had nearly disappeared. The two absorption peaks near 1300–1400 cm^{-1} and 1550–1750 cm^{-1} were similar to the characteristic peaks of graphene, which were caused by C=O, C–O–C, C–OH and the stretching vibration of C=C of the graphite crystal sp^2 structure, respectively. The intensity of the O–H stretching vibration peak near 3500 cm^{-1} was significantly

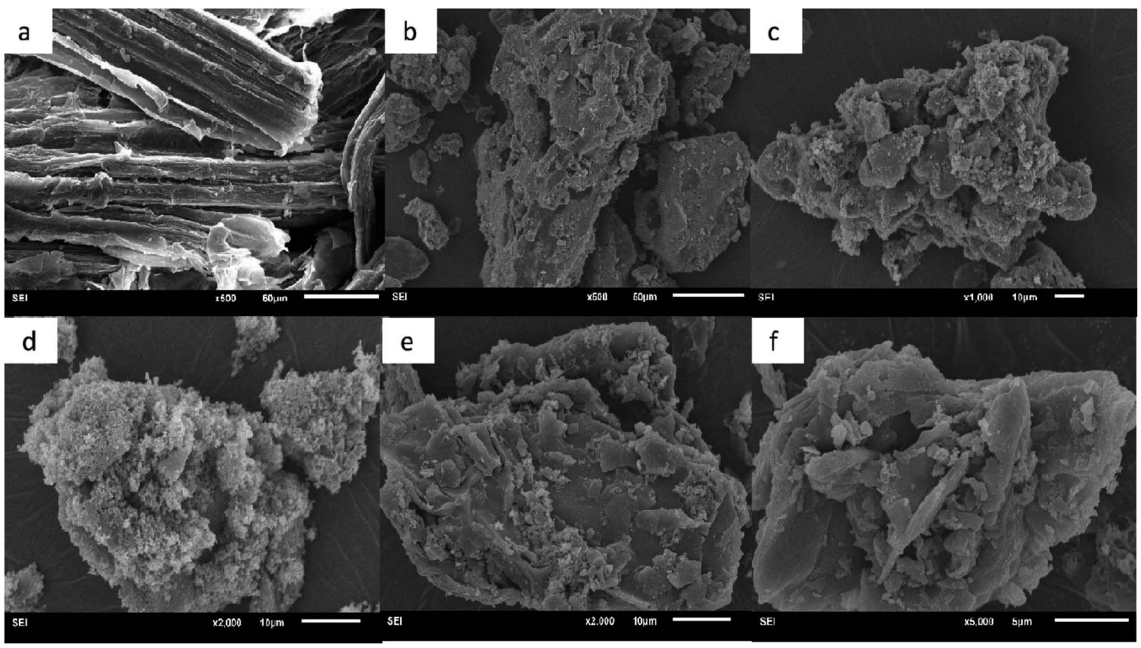

Fig. 10 SEM images: the corn straw (a), graphitized carbon directly prepared from corn straw (b and c), graphitized carbon wrapped by the annealed and cooled iron element before iron element removal (d), graphitized carbon after pickling with different magnifications (e and f).

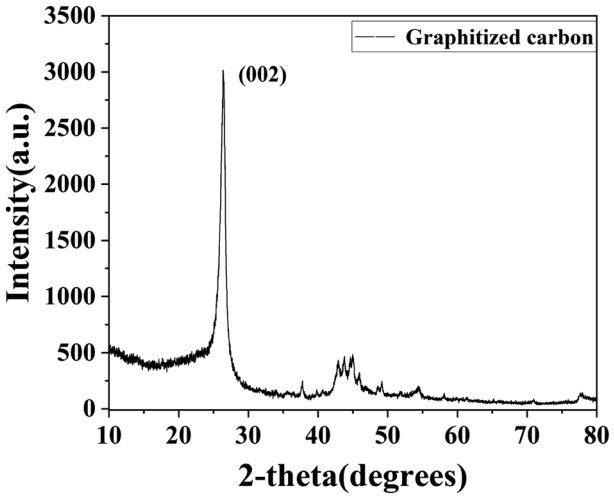

Fig. 11 X-ray diffraction patterns of graphitized carbon.

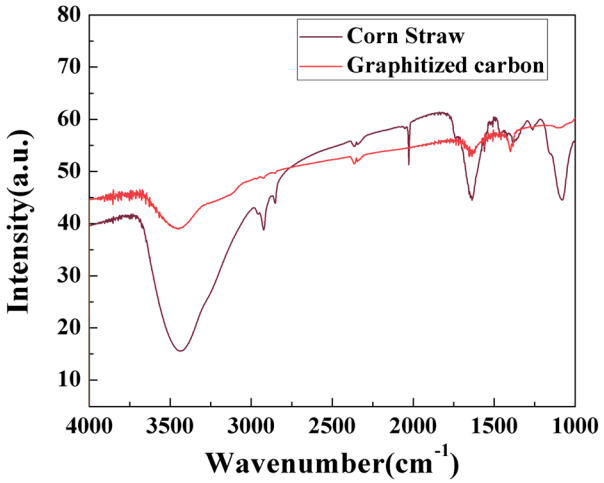

Fig. 12 Infrared spectra of the corn straw and graphitized carbon.

weaker because the hydroxyl groups in the corn straw were re-polymerized by phosphoric acid and polyols to form water molecules (H_2O) or other small molecules at the late stage of liquefaction. After graphitization, the absorption waveform state converged to the characteristic peak of graphene. Hydrogen bonds were probably formed, which are favorable for counteracting the van der Waals forces between the graphene layers.

5 Conclusion

This study utilized a combination of liquefaction–carbonization–graphitization technology innovation through qualitative and quantitative analysis, a solid–liquid ratio of corn straw powder and liquefied agent of 1 : 2, carbonization temperature of 600 °C, graphitization temperature of 850 °C, ferric acetylacetonate as the graphitization catalyst, and the catalyst concentration was 7.0 mmol g^{-1}. Corn straw-based graphitized carbon showing a better graphitization degree, microscopic lamellar structure, and smaller defects was successfully prepared. The resulting proposed mechanism of the graphitized carbon process from corn straw provides a practical pathway for the preparation and utilization of corn straw to high-quality materials.

Ethical approval

This article does not contain any studies with human participants or animals performed by any of the authors.

Conflicts of interest

We declare that we have no conflicts of interest to this work. We do not have any commercial or associative interest that represents a conflict of interest in connection with the work submitted.

Acknowledgements

This work was supported by Jilin Province Science and Technology Department (grant number 20220101074JC); Climbing Project Fund of Changchun University (grant number ZKP202121).

References

1 H. Chang, *Biomass conversion and utilization*, Science Press, Beijing, 2019.
2 H. Miao, *J. Phys.: Conf. Ser.*, 2022, **2152**, 012053.
3 X. Zhu, G. Li and T. Qin, *J. Nanjing For. Univ.*, 2014, **38**, 157–162.
4 X. Li, X. Li, W. Li, T. Lei, J. Shi, Z. Wang and X. Duan, *J. Beihua Univ.*, 2018, **19**, 108–113.
5 B. Wei, F. Chen, Z. Li and Y. Cheng, *Chem. Ind. For. Prod.*, 2014, **34**, 53–59.
6 R. Briones, L. Torres, Y. Saravia, L. Serrano and J. Labidi, *Ind. Crops Prod.*, 2015, **78**, 19–28.
7 T. H. Pedersen, I. Grigoras, J. Hoffmann, S. S. Toor, I. M. Daraban, C. U. Jensen, S. Iversen, R. Madsen, M. Glasius and K. R. Arturi, *Appl. Energy*, 2016, **162**, 1034–1041.
8 P.-G. Duan, S.-K. Yang, Y.-P. Xu, F. Wang, D. Zhao, Y.-J. Weng and X.-L. Shi, *Energy*, 2018, **155**, 734–745.
9 J. R. Collett, J. M. Billing, P. A. Meyer, A. J. Schmidt, A. B. Remington, E. R. Hawley, B. A. Hofstad, E. A. Panisko, Z. Dai and T. R. Hart, *Appl. Energy*, 2019, **233**, 840–853.
10 H. Jiang, F. Deng, Y. Luo, Z. Xie, Y. Chen, P. Zhou, X. Liu and D. Li, *J. Cleaner Prod.*, 2022, **353**, 131682.
11 W. Zhang, Z. Wang, T. Ge, C. Yang, W. Song, S. Li and R. Ma, *Korean J. Chem. Eng.*, 2022, **39**, 1240–1247.
12 B. N. Tochi, Z. Wang, S.-Y. Xu and W. Zhang, *Pak. J. Nutr.*, 2009, **8**, 1184–1189.
13 R. Zeng, X.-Y. Yin, T. Ruan, Q. Hu, Y.-L. Hou, Z.-Y. Zuo, H. Huang and Z.-H. Yang, *Bioengineering*, 2016, **3**, 13.

14 B. Zhang, Y. Gao, L. Zhang and Y. Zhou, *J. Integr. Plant Biol.*, 2021, **63**, 251–272.
15 X. Li, X. a. Xie, C. Zheng and Y. Li, *Trans. Chin. Soc. Agric. Eng.*, 2011, **27**, 119–124.
16 C.-Y. Zheng, X.-A. Xie, H.-X. Tao, L.-S. Zheng and Y. Li, *J. Fuel Chem. Technol.*, 2012, **40**, 526–532.
17 J. Sun, Y. L. Wang, X. A. Xie, L. I. Wei, L. I. Lu, L. I. Yan, D. Fan and X. Wei, *J. Fuel Chem. Technol.*, 2017, **45**(6), 660–668.
18 N. Singh, M. Sharma, D. Mondal, D. A. Maru and K. Prasad, *Mater. Sci. Energy Technol.*, 2021, **4**, 100–106.
19 Q. Chen, J. Gu, K. Sun, C. Zhang and S. Tian, *Polym. Mater.: Sci. Eng.*, 2013, **29**, 125–128.
20 D. Y. Qi, *Preparation and properties of biomass-based polyether polyols(D)*, Changchun University of Technology, 2020.
21 T. Yelverton, A. T. Brashear, D. G. Nash, J. E. Brown and P. Burnette, *Fuel*, 2020, **264**, 116774.
22 X. Wang, A. Dong, Y. Hu, J. Qian and S. Huang, *Chem. Commun.*, 2020.
23 A. Jorio, R. Saito, G. Dresselhaus and M. S. Dresselhaus, *Raman Spectroscopy in Graphene Related Systems [M]*, Wiley-VCH, 2011.
24 W. Lei, *The designed synthesis electrochemical performances of crystaline nanocarbon-based composites*, Jilin University, 2013.
25 F. Gu, J. Ma and C. Che., *J. Chin. Cereals Oils Assoc.*, 2022, **37**, 240–245.